Two contrastive rapid recrystallization mechanisms revealed in practically used phase-change recording materials

T. Matsunaga[1,2],   J. Akola[3,4,5], S. Kohara[2,6], T. Honma[6], K. Kobayashi[7], E. Ikenaga[6], R. O. Jones[3,8] , N. Yamada[1,2] * , M. Takata[2,6,9,10] and R. Kojima[1]

[1]Panasonic Corporation, 3-1-1 Yagumo-Nakamachi, Moriguchi, Osaka 570-8501, Japan / [2]JST, CREST, 5 Sanbancho, Chiyoda-ku, Tokyo 102-0075, Japan / [3]Institut für Festkörperforschung, Forschungszentrum Jülich, D-52425 Jülich, Germany / [4]Nanoscience Center, Department of Physics, University of Jyväskylä, PO Box 35, FI-40014 Jyväskylä, Finland / [5]Department of Physics, Tampere University of Technology, PO Box 692, FI-33101 Tampere, Finland / [6]Japan Synchrotron Radiation Research Institute (SPring-8), 1-1-1 Kouto, Sayo-cho, Sayo-gun, Hyogo 679-5198, Japan / [7]Beamline Station at SPring-8, National Institute for Materials Science, 1-1-1 Kouto, Sayo-gun, Hyogo 679-5198, Japan / German Research School for Simulation Sciences, FZ Jülich and RWTH Aachen University, D-52425 Jülich, Germany / RIKEN SPring-8 Center, 1-1-1 Kouto, Sayo-cho, Sayo-gun, Hyogo 679-5148, Japan / Department of Advanced Materials, University of Tokyo, Chiba 277-8561, Japan.

ABSTRACT

Today, the most common phase-change materials are $GeTe$-Sb_2Te_3 pseudobinary compounds and Sb-Te binary compounds with small amounts of In, Ag and/or Ge. These materials possess sufficiently fast recrystallization speed; however, recrystallization in the two materials is strikingly different, although their crystal structures are very similar to each other. In the former material, the recrystallization begins all at once from uncountable crystalline fragments embedded in the amorphous mark; whereas in the latter materials it starts from the rim of the mark and moves toward the center of the mark through bond interchanges in the atomic network.

Key words: Ge-Sb-Te, Ag-In-Sb-Te, DFT, RMC, amorphous, crystal, phase change

1. INTRODUCTION

Phase change recording is now extensively used for high density non-volatile memories [1]. Since 1970s, various materials have been proposed for the purpose, and today we have obtained two superior materials of $GeTe$-Sb_2Te_3 (GST) [2] and Sb-Te based alloys such as AIST (Ag-In-Sb-Te quadruple compounds) [3]. These compounds possess two indispensable features for data storage; i.e., high endurance of the amorphous phase and high-speed phase change from the amorphous to the crystalline phase. Their recrystallization speeds are sufficiently fast; however, their phase-change processes are strikingly different; although their crystal structures are very similar to each other (they have octahedral coordination structures formed by the p-p bonding [4], [5], [6]). It is well known that in the former group recrystallization proceeds mainly by way of nucleation inside the marks, in the latter group by way of crystal growth from the rim [6]. There have been numerous studies on amorphous GST (a-GST); on the other hand, little is known about the structures of a-AIST. In order to clarify this difference, we analyse the structure of the AIST amorphous phase through several x-ray analyses and DFT calculations. We believe that this investigation will give us an important clue to develop new phase-change materials in the next generation.

2. EXPERIMENTS

The $Ag_{3.5}In_{3.8}Sb_{75.0}Te_{17.7}$ powder specimens for the XRD experiment were made by laminating a 5-nm-thick ZnS–SiO_2 film on a glass disc (diameter 120 mm) and sputtering to form a recording film of thickness 200–500 nm. The specimen was removed from the glass substrate using a spatula, and its composition was studied using inductively coupled plasma atomic emission spectrometry.

The specimens for the EXAFS experiments were made by laminating a Kapton film of 25 µm thickness overlaid

on a glass disc with a diameter of 120 mm, followed by sputtering to form the recording films of thickness 300 nm. XRD measurements confirmed that the films were amorphous. The Kapton film sheets were peeled from the glass discs and cut into 10 mm squares, which were then stacked to form the specimens. The EXAFS measurements were carried out at the BL14B2 bending-magnet beamline of SPring-8. The incident X-ray beam was monochromatized by a Si double-crystal monochromator with (111) net planes. Contamination with higher harmonics in the incident beam was removed by rhodium-coated mirrors located downstream of the monochromator. Vertical focusing of the incident beam at the sample was performed by slightly bending the mirrors. EXAFS data of Ag, In, Sb and Te K edges were collected in transmission mode at 26 K. The backscattering amplitudes and the mean free paths used for the EXAFS analyses were obtained from FEFF [7] calculations. The coordination numbers N and bond lengths r were determined by least-squares fitting using the Rigaku REX2000 software [8]. The analysis was simplified by assuming that each absorbing atom was surrounded by Sb atoms alone.

The XRD experiments were carried out at room temperature at the SPring-8 high-energy XRD beamline BL04B2 [9] using a two-axis diffractometer dedicated to glass, liquid and amorphous materials. The incident X-ray energy was 61.5 keV. The diffraction patterns of the powder sample in a thin-walled (10 mm) tube of 0.5 mm diameter (supplier: GLAS Müller, 13503 Berlin, Germany) and an empty tube were measured in transmission geometry. The intensity of incident X-rays was monitored by an ionization chamber filled with Ar gas, and the scattered X-rays were detected by a Ge detector. A vacuum chamber was used to suppress the air scattering around the sample, and the data collected were corrected using a standard program [9].

3. RESULTS

EXAFS analysis

Our EXAFS measurements performed at various temperatures revealed that the a-AIST defends its atomic configuration against rise in temperature. We analysed the local structures in this amorphous material at several temperatures from 10 K to 300 K by the EXAFS method under the assumption that the four kinds of constituent atoms are all surrounded only by Sb atoms, because Sb is the main element of this material (and besides, atomic numbers of these four atoms are very close to each other, which makes it very difficult for us to distinguish these atoms in the x-ray analyses). The structural parameters, coordination number N, bond length r, Debye-Waller factor B etc. were obtained by least squares curve fitting [8]. Figure 1 shows the temperature dependence of the Debye–Waller factors (In this figure, those are shown by transformed into B.), which represent the dynamic and static shifts (fluctuation) their equilibrium positions. As can be seen in this figure, Bs gradually increase with temperature raise; however, their slopes are fairy gentle, which is remarkable when compared with those for the crystalline phase [5]. We learned above that the atomic configuration and the bond lengths remain almost unchanged without depending on temperature. In addition to this, it has been revealed that the dependence of the atomic fluctuation on temperature is considerably small. These two mean that the structure of the amorphous phase is stable enough probably even in the high temperatures below the transition temperature, which is presumed to enable this amorphous material to retain its structure for a sufficiently long time, especially around room temperature or lower. This structural feature of the amorphous phase is probably due to the strong covalent bondings of the atoms. As shown below, DF-RMC analysis revealed in fact that Sb atoms have 3 (short) +3 (long) coordination structures both in the crystalline and amorphous phases; however, in the latter phase, the bond length of the former is considerably shorter than that in the crystalline phase. We can therefore regard the coordination number of Sb as approximately three, which satisfies the 8-N rule [10]. This bonding nature is presumed to be a major reason that this amorphous material shows a sufficient endurance at room temperature, as well as the amorphous GST [11], [12].

DF-RMC analysis

As it is well known, molecular dynamics (MD) is a computer simulation of physical movements of atoms and molecules, and density-functional theory (DFT) is currently a very useful, another computational analysis method for examining structural, electronic, and dynamical properties in materials science. The combination of these two methods, molecular dynamics (MD) based on DFT makes it possible for us to study dynamical processes such as structural transformations of covalently bonded materials as well as chemical reactions in condensed matters. On the other hand, the Reverse Monte Carlo (RMC) simulation is also very useful to experimentally examine amorphous structures [9].

However, it is ordinary difficult for us to analyze the actual structure of an amorphous material from only one dimensional diffraction data. Besides that, the presence of four elements in AIST and the dominance of two (Sb, Te) with similar atomic numbers make it further difficult to determine the local structure by XRD alone. We then this time scrutinized the amorphous structure by using the combination of density functional (DF)–molecular dynamics (MD) and reverse Monte Carlo (RMC) simulations to reproduce X-ray diffraction (XRD), and furthermore, hard X-ray photoelectron spectroscopy (HXPS) data [6].

The determined structure is shown in Fig.2 together with that of GST225 ($Ge_2Sb_2Te_5$). These results agree with those found in the EXAFS analyses. Table 1 also gives values for the DF-RMC geometry on the basis of the partial pair distribution functions and bond-order analysis [6]. The coordination numbers obtained from EXAFS measurements for Sb and Te (3.7±0.3 and 2.4±0.4, respectively) agree well with the calculated values. The EXAFS measurements indicate that there are only small differences between the bond lengths, with Ag bonds being slightly shorter (2.77 Å). This is consistent with the DF-RMC results, where the bond lengths are near 2.85±0.05 Å for most pair distribution functions. As mentioned above, the coordination number of Sb approximately satisfies the 8-N rule [10]; however, it connects with other three at longer distance. We stress that Sb atoms in the amorphous phase have 3+3 coordination structures as well as in the crystalline phase as seen in Fig. 3(b).

Figure 4 shows the structure factors $S(Q)$ of AIST and GST obtained using XRD. The crystalline forms of both have sharp Bragg peaks (red lines), and the amorphous forms (black lines) have typical halo patterns. However, oscillations up to the maximum Q value in a-AIST indicate a structure with well defined short-range order. Fourier transformation of the $S(Q)$ leads to the total correlation functions $T(r)$ for c-GST and c-AIST (Fig. 2b), which are very similar beyond 4 Å. Small differences between the two crystalline forms are found at shorter distances, for example the double peak in c-AIST (2.93 Å and 3.30 Å) and a single peak in c-GST (2.97 Å). The $T(r)$ for the amorphous materials, however, are significantly different: the first peak in a-AIST (2.86 Å) is only slightly shorter than that found in c-AIST (2.93 Å), whereas the first peak in a-GST (2.79 Å) is much shorter than that in c-GST (2.97 Å). We note also that the shoulder on the second peak in a-AIST (3.5 Å, arrowed) is near that observed in the crystalline form (3.30 Å). The pronounced difference between the diffraction patterns of the two materials is strong evidence that they crystallize differently. The atomic motion and/or diffusion accompanying the PC are larger in GST than in AIST, where the PC is accompanied by small changes in bond lengths.

4. DISCUSSION

Phase-change in GST materials

It is well known that the most commonly used recording material today is GeTe-Sb_2Te_3 pseudobinary compound. A recording film made of this material can be switched rapidly and reversibly between the crystalline phase and the amorphous phase by a brief laser irradiation (several tens of nanoseconds). This pseudobinary compound maintains the same NaCl-type structure (space group : $Fm\bar{3}m$) over a wide range of compositions from 100 % of GeTe to at least $(GeTe)_1(Sb_2Te_3)_2$ (namely, $Ge_1Sb_4Te_7$) when subjected to instantaneous heating by laser irradiation followed by equally rapid cooling (see Fig. 3(a)) [4]. In this structure, the Cl:4a site is completely occupied by Te atoms, whereas the Na:4b site is randomly occupied by Ge and Sb atoms and vacancies. When the chemical formula of the pseudobinary compound is expressed as $(GeTe)_x$-$(Sb_2Te_3)_{1-x}$; $(0 \leq x \leq 1)$, the ratio of the vacancy continuously changes according to $(1-x)/(3-2x)$. The atoms in the crystals are orthogonally connected with six adjacent atoms (or vacancies) by p-p bonding; the atomic network of this structure consists of fourfold and sixfold rings. The atomic arrangement of the amorphous phase can be geometrically obtained by minute shifting of the atoms in random directions almost without bond interchanges found in the phase change of AIST (this is shown below), which means that, when an amorphous GST is given energy by laser irradiation (or ohmic heating) and then instantaneously cooled, the atomic migration distance is so short that the solid instantaneously crystallizes into this type of highly symmetric (spatially isotropic) structure.

Many structural investigations have been dedicated to the GST amorphous materials. Coordination numbers for three constituent atoms approximately follow the 8-N rule, largely different from those of the crystalline phase; for instance, those of a-GST225 are ca 3.7, 3.0, and 2.6 around Ge, Sb, and Te atoms respectively. These approximately

satisfy the 8-*N* rule, showing the characteristics of covalent bonds often observed in calcogenide amorphous materials. The bond lengths are also shorter than in the crystalline phase. The atomic configuration is maintained almost unchanged up to the transition temperature to the crystalline phase [11], [12]. It has been considered that such a strong covalent bonding nature gives these amorphous materials sufficient endurance, namely, long-term data preservation. These GST materials contain three kinds of atoms, Ge, Sb, and Te; which means that, if these atoms connect with each other with equal probability in their amorphous structures, six kinds of atomic pairs should be found at the ratio provided by a random covalent network model. It has been revealed, however, that these amorphous materials comprise a large number of Ge-Te and Sb-Te atomic pairs beyond the above estimation (Note that the crystalline phase is formed by these two pairs as well). In a-GST225, 40% of the rings are fourfold or sixfold and a considerable amount of the relict $GeTe_4$ tetrahedra and $SbTe_3$ pyramids whose bond angles are distributed around 90º as same as those of the crystalline phase [13], [14]; we can find even NaCl-type crystalline fragments in the amorphous atomic network as seen in Fig. 2(a). Once sufficient heat energy is supplied to the amorphous material; however, those crystalline fragments act as first nuclei to crystallize their surroundings all at once. We presume that this is the rapid phase-change mechanism of the GST materials. However, in addition to these countless nuclei, a large number of huge voids are present in the amorphous body, which impedes smooth crystal growth. As a result, the texture of the crystallization-completed amorphous mark shows a mosaic pattern inlaid by a large number of tiny crystallites with 10 - 20 nm diameters. In addition, amorphous and crystalline GST materials have considerably low thermal conductivities, meaning that these materials can locally heat up at once by laser irradiation or ohmic heating [12]. This feature is very favorable to cause rapid phase change.

Phase-change in AIST materials

Laser-annealed $Ag_{3.5}$ $In_{3.8}$ $Sb_{75.0}$ $Te_{17.7}$ crystallizes into an *A*7 structure, as do As, Sb and Bi [5]. The *A*7 structure [15] is shown in Fig. 3(b). Four constituent atoms randomly occupy 6(*c*) 0, 0, *z* of space group $R\overline{3}m$. As seen in the figure, there are three shorter interatomic distances (r_s) shown by black lines and three longers (r_l) shown by gray lines between the central atom and its six neighbors, and two kinds of hexahedrons which forms a geometric unit. One of the hexahedrons (A-B) is compressed along the threefold rotation-inversion axis and the other (B-C) is expanded. Both of them can be regarded as a slightly distorted cube. This crystal can be described as a Jahn-Teller deformed structure to stabilize the electronic structure showing a semi-metallic feature [16], which can be regarded almost as a semiconductor. However, as mentioned above, the atoms in the crystal are quasi-orthogonally connected with adjacent six atoms (3+3 octahedron) by p-p bonding as well as a NaCl-type GST crystal; the atomic network of this structure consists of fourfold and sixfold rings. The densities of states (DOS) of both crystals are very similar to each other. Green arrows in the Fig. 5 show resultant vectors of short bonds, which are parallel to each other and arranged along the *c*-axis direction. The structure (bond lengths and angles) and chemical coordination numbers obtained by the RMC-refined DF calculations lead to the local environment around Sb atoms shown in Fig. 5. Both a-AIST (left panel) and c-AIST (right panel) resemble a (distorted) 3 + 3 octahedron.

In the amorphous state, interatomic distance between the central atom and three shorter coordination atoms is considerably shorter than in the crystalline state; they are connected to each other by a stronger covalent force than those in the crystal to form isolated molecule by themselves. These molecules are weakly connected by vertices or edges; a spatially periodic arrangement is not required of them. For this reason, the green arrows are randomly oriented as seen in the left bottom panel of Fig. 5. However, once sufficient heat energy is given to the amorphous material, it causes interchange of one bond in a 3+3 coordination octahedron to rearrange, parallel neighboring two vectors. This rearrangement swiftly propagates from neighbor to neighbor forming the crystalline preferred orientation, which finally shows needle-like crystallization texture from the rim toward the center of the mark. Fortunately for the growth dominated recrystallization materials, few voids to retard smooth crystal growth were found in the amorphous AIST.

Roll of small number of elements, Ag and In, in the AIST material

Sb-Te is the mother alloy for the AIST materials. The diffraction patterns obtained for the sputtered Sb_8Te_3 film, which is one of these alloys, are shown in Fig.6. During the heating process (Fig. 6(a)), these profiles indicated that the as-sputtered Sb_8Te_3 specimen was in an amorphous state at room temperature, but crystallized with heating into a

transient homologous structure close to the A 7-type. However, this is not just the A7-type structure but has already crystallized into a complicated structure with a long period. After that, a sufficient heat treatment gives this material its original, $11R$ - $(Sb_2)_3(Sb_2Te_3)_1$ structure at around 830 K. However, as mentioned above, Sb-Te alloys with the dopants, Ag and In, crystallize into real A7-type structures by instantaneous laser annealing (Figs. 3(b) and 6(b)). This structure of the quadruple compound is surprisingly stable; it is kept up to near the melting points. It is therefore concluded that these elements work to hold the crystal in a simple and an isotropic structure. We presume that presence of simple and isotropic crystalline phase is one of requisite features for high-speed phase-change materials; for it is considered that atomic arrangements of the amorphous phase can be transformed into that crystalline phase through minimal atomic shifts.

5. SUMMARY

According to the bond-interchange model, crystallization of a-AIST can be viewed as a rapid succession of diffusionless events where the 3 + 3 octahedra are aligned along the crystalline c axis imposed by the surrounding crystal (see Fig. 5). Heating or photon excitation causes the octahedra to align near the matrix boundary, and blade- or needle-like crystallites can grow along the laser- scanning direction, as often observed in Sb-based PC materials. The lack of cavities and chemical alternation in a-AIST favor smooth crystal growth. On the other hand, in the latter material, GST, high-speed phase change begins from uncountable crystalline fragments embedded in the amorphous network all at once. In the former material, Sb atoms are generally surrounded by Sb atoms of the same kind (with the same coordinate bonding nature); whereas in the latter material, neighboring atom of Sb is almost always Te. This is presumed to be one major reason that the former materials can take place such a bond-interchange phase transition.

REFERENCES

[1]   M. Wuttig and N.Yamada: *Nat. Mater*. **6**, 824 (2007).
[2]   N. Yamada, E. Ohno, K. Nishiuchi, and N. Akahira, *J. Appl. Phys*. **69**, 5, 2849 (1991).
[3]   H. Iwasaki, Y. Ide, Y. Harigaya, Y. Kageyama, and I. Fujimura: *Jpn. J. Appl. Phys. Series 6 Proc. Int. Symp. on Optical Memory* **68** (1991).
[4]   T. Matsunaga, R. Kojima, N. Yamada, K. Kifune, Y. Kubota, Y. Tabata, and M. Takata: *Inorg. Chem.* **45**, 2235 (2006).
[5]   T. Matsunaga, Y. Umetani, and N. Yamada: *Physical Review B* **64**, 184116 (2001).
[6]   T. Matsunaga, J. Akola, S. Kohara, T. Honma, K.Kobayashi, E. Ikenaga, R. Jones, N. Yamada,   M.Takata and R. Kojima: *Nat. Mater.* **10**, 129 (2011).
[7]   A. L. Ankudinov, B. Ravel, J. J. Rehr, and S. D. Conradson: *Phys. Rev. B* **58**, 7565 (1998).
[8]   T. Taguchi, T. Ozawa, and H. Yashiro, H. REX2000: *Phys. Scr.* **T115**, 205 (2005).
[9]   S. Kohara, M. Itou, K. Suzuya, Y. Inamura, Y. Sakurai, Y. Ohishi, and M. Takata: *J. Phys. Condens. Matter* **19**, 506101 (2007).
[10] N. F. Mott: *Philos. Mag.* **19**, 835 (1969).
[11] T. Matsunaga, R. Kojima, N. Yamada, and M. Takata: *Europian¥Phase Change and Ovonics Symposium 2008*, http://www.epcos.org/library/library2008.htm
[12] T. Matsunaga, N. Yamada, R. Kojima, S. Shamoto, M. Sato, H. Tanida, T. Uruga, S. Kohara, M. Takata, P. Zalden, G. Bruns, I. Sergueev, H. C. Wille, R. P. Hermann, M. Wuttig: *Adv. Funct. Mater.* **21**, 12, 2232 (2011).
[13] S. Kohara, K. Kato, S. Kimura, H. Tanaka, T. Usuki, K. Suzuya, H. Tanaka, Y. Moritomo, T. Matsunaga, N. Yamada, Y. Tanaka, H. Suematsu, and M. Takata, *Appl. Phys. Lett.* **89**, 201910 (2006).
[14] J. Akola, R. O. Jones, S. Kohara, S. Kimura, K. Kobayashi, M. Takata, T. Matsunaga, R. Kojima, and N. Yamada: *Phys. Rev. B* **80**, 020201 (2009).
[15] G. L. Clark: *Applied X-rays* (McGraw-Hill, 1955)
[16] R. Hoffmann: *Solids and Surfaces: A Chemist's View of Bonding in Extended Structures* (Wiley-VCH, 1989).

Biographyies

Dr. Toshiyuki Matsunaga received his Ph.D. in physics for his work on crystal structures, phase transitions, and bonding natures in intermetallic compounds in 1986 from Hiroshima University in Japan. Since joining Matsushita

Electric Industrial in 1984, he has developed new electronic devices by analyzing a large number of materials by such surface analysis methods as SEM, XMA, AES, SIMS, and TPD. Since 1996, he has been involved in optical disc R and D, concentrating on basic transition phenomenon research in phase-change recording materials.

Table 1   Local structure of a-AIST determined by EXAFS at 26 K and DF / MD calculations. N, coordination number; r, nearest-neighbour bond length; N_{bond}, chemical coordination number. Theoretical values from RMC-refined DF geometry (N_{DF-MD} and r_{DF-MD}) and chemical bond-order analysis. The N_{bond} values of c-AIST are given in parentheses.

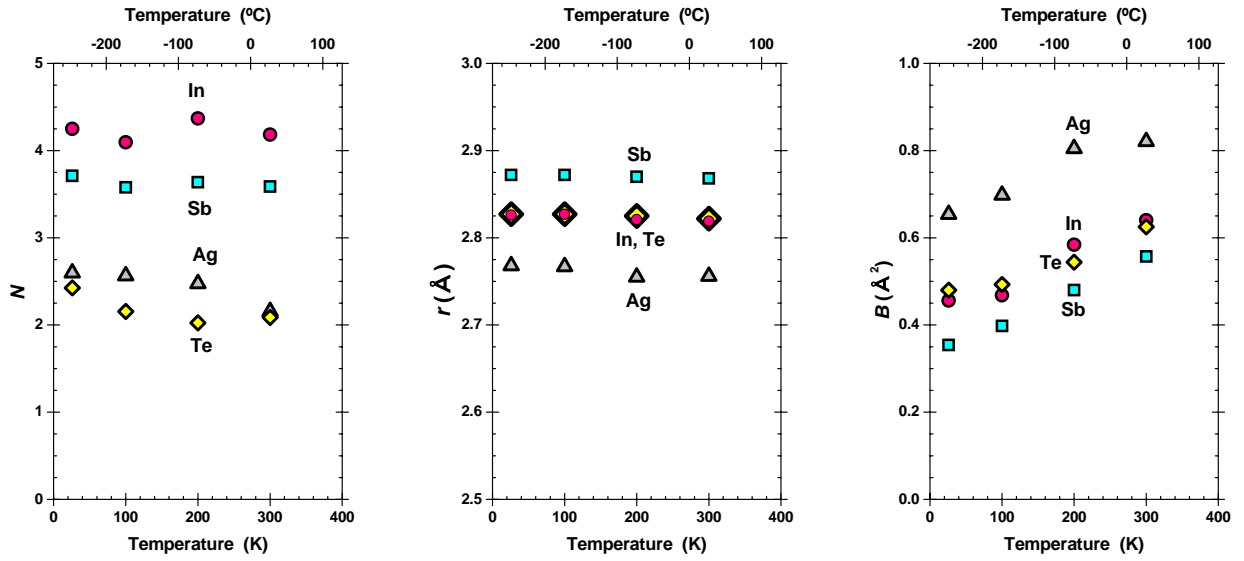| Atom	N	r (Å)	$N_{DF/MD}$	$r_{DF/MD}$ (Å)	N_{bond}
Ag	3.3 ± 0.5	2.768 ± 0.006	4.4	2.80 ± 0.05	1.9 (2.0)
In	4.3 ± 0.6	2.826 ± 0.006	3.1	2.85 ± 0.05	2.5 (2.9)
Sb	3.7 ± 0.3	2.872 ± 0.006	3.3	2.85 ± 0.05	3.1 (3.2)
Te	2.4 ± 0.4	2.827 ± 0.006	2.5	2.85 ± 0.05	2.5 (2.6)

Fig. 1.   Temperature dependences of the coordination numbers N, bond lengths r, and temperature factors (the atomic displacement parameters) B for the amorphous $Ag_{3.5} In_{3.8} Sb_{75.0} Te_{17.7}$.
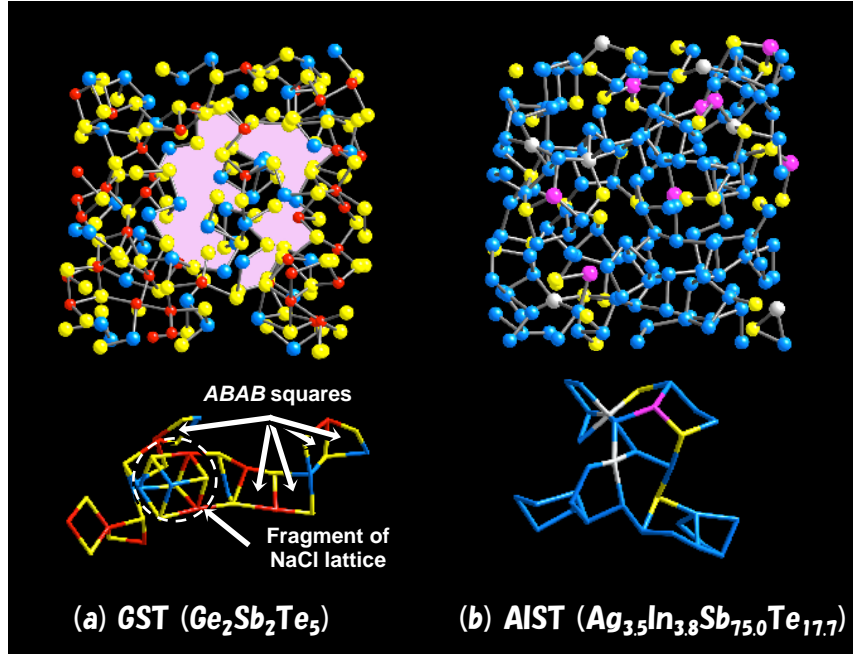
Fig. 2   (a) Section of 460-atom DF-MD model of a-GST (24 Å × 24 Å × 12 Å). Ge, red; Sb, blue; Te, yellow; large cavity, pink. (b) Section of 640-atom DF-MD model of -AIST (24 Å × 24 Å × 12 Å). Ag, silver; In, magenta; Sb, blue; Te, yellow. A large cavity is present among the atomic arrangement in the a-GST structure. Enlarged configuration (left bottom figure) shows that a-GST has many structural units (ABAB-squares) with alternating Te and Ge (or Sb) atoms. We can observe even a fragment of NaCl lattice. On the other hand, few cavities are observed in the a- AIST structure on the right.
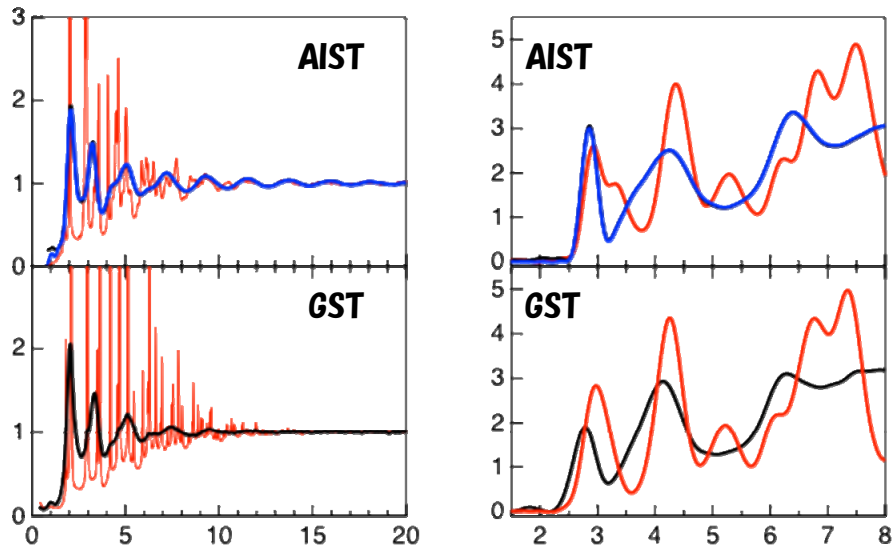

Fig. 4.   HXRD data for AIST and GST, and atomic configurations of a-AIST and a-GST. (a) Structure factors $S(Q)$ and (b) total correlation functions $T(r)$ of AIST and GST. Red line, experimental data of crystalline phase; black line, experimental data of amorphous phase; blue line, DF-RMC model of a-AIST. The DF-RMC and experimental results are practically indistinguishable.

Let's assume that bonding electrons are interchanged between the two bond pointed by the yellow arch,

hν
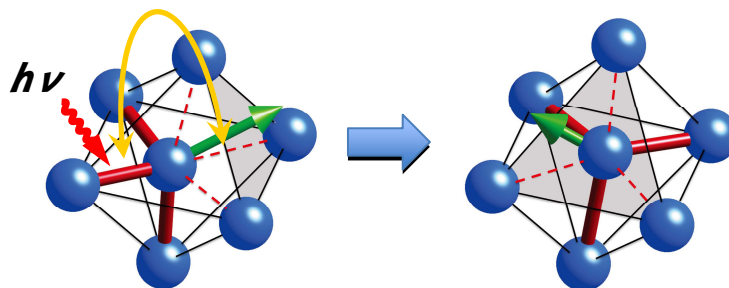
which changes the direction of the orientation vector shown in green.
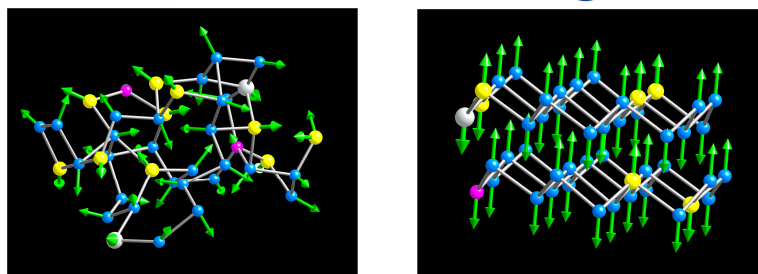
Fig. 5.   The bonding electrons are excited by laser light, causing the atoms in the amorphous phase to move. Finally, the central atom with three short (red) and three long (dashed) bonds crosses the center of the distorted octahedron, interchanging a short and a long bond. Green: resultant vector of short bonds. Resonant bonding between periodic short and long bonds leads to the crystalline A7 network. The grey sticks (lower right) correspond to the red bonds (upper right). Atom colors as in Fig. 2(b).
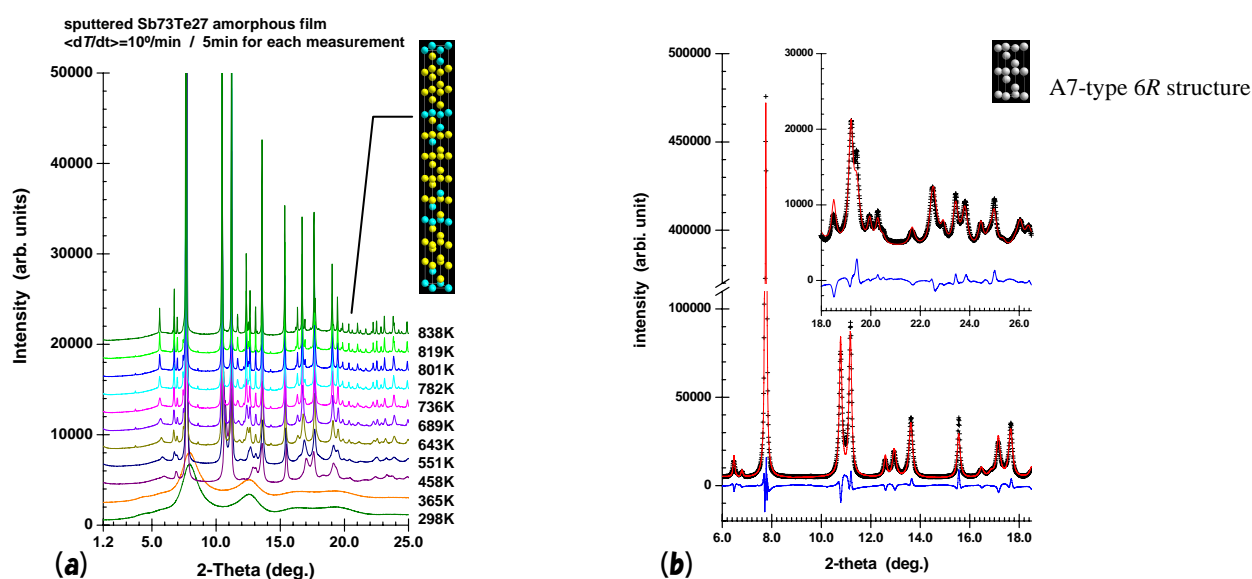

Fig. 6.   (a) Temperature dependence of the X-ray powder diffraction profiles of an Sb_8Te_3 powder specimen. These profiles indicated that the as-sputtered Sb_8Te_3 specimen was in an amorphous state at room temperature, but crystallized with heating into a transient homologous structure close to the A 7-type. As temperature rises, the layer period of the structure gets longer to attain its original structure at around 830 K. The inset shows the projection of this final structure ($11R$) onto a 3D-section: the atomic positions (Sb:yellow, Te:blue). (b) X-ray diffraction pattern of laser-crystallized $Ag_{3.4}In_{3.7}Sb_{76.4}Te_{16.5}$, one of AIST compounds, at room temperature. The Rietveld analysis revealed that this quadruple compound has an A7-type structure ($6R$). Observed and calculated patterns are represented by + marks and red lines. A difference curve (observed – calculated) appears at the bottom of each panel in blue. Addition of Ag and In to Sb-Te makes its crystal structure simpler and spatially more isotropic.